

Interplay between mass-impurity and vacancy phonon scattering effects on the thermal conductivity of doped cadmium oxide

Brian F. Donovan, Edward Sachet, Jon-Paul Maria, and Patrick E. Hopkins

Citation: [Applied Physics Letters](#) **108**, 021901 (2016); doi: 10.1063/1.4939652

View online: <http://dx.doi.org/10.1063/1.4939652>

View Table of Contents: <http://scitation.aip.org/content/aip/journal/apl/108/2?ver=pdfcov>

Published by the [AIP Publishing](#)

Articles you may be interested in

[Hydrogen-doped In₂O₃ transparent conducting oxide films prepared by solid-phase crystallization method](#)
J. Appl. Phys. **107**, 033514 (2010); 10.1063/1.3284960

[Relationship between the cathodoluminescence emission and resistivity in In doped CdZnTe crystals](#)
J. Appl. Phys. **106**, 044901 (2009); 10.1063/1.3197031

[Vacancy phonon scattering in thermoelectric In₂Te₃ – InSb solid solutions](#)
Appl. Phys. Lett. **94**, 122112 (2009); 10.1063/1.3109788

[Transparent conducting zinc oxide thin films doped with aluminum and molybdenum](#)
J. Vac. Sci. Technol. A **25**, 955 (2007); 10.1116/1.2735951

[Strain field fluctuation effects on lattice thermal conductivity of ZrNiSn -based thermoelectric compounds](#)
Appl. Phys. Lett. **85**, 1140 (2004); 10.1063/1.1783022

A promotional banner for Applied Physics Reviews. On the left is a small image of a journal cover titled 'AIP Applied Physics Reviews' showing a diagram of a layered structure. The main text reads 'NEW Special Topic Sections' in large white letters. Below this, it says 'NOW ONLINE' in yellow, followed by 'Lithium Niobate Properties and Applications: Reviews of Emerging Trends' in white. The AIP Applied Physics Reviews logo is in the bottom right corner.

NEW Special Topic Sections

NOW ONLINE
Lithium Niobate Properties and Applications:
Reviews of Emerging Trends

AIP Applied Physics Reviews

Interplay between mass-impurity and vacancy phonon scattering effects on the thermal conductivity of doped cadmium oxide

Brian F. Donovan,¹ Edward Sachet,² Jon-Paul Maria,² and Patrick E. Hopkins^{3,a)}

¹*Department of Materials Science and Engineering, University of Virginia, Charlottesville, Virginia 22904, USA*

²*Department of Materials Science and Engineering, North Carolina State University, Raleigh, North Carolina 27695, USA*

³*Department of Mechanical and Aerospace Engineering, University of Virginia, Charlottesville, Virginia 22904, USA*

(Received 4 August 2015; accepted 26 December 2015; published online 12 January 2016)

Understanding the impact and complex interaction of thermal carrier scattering centers in functional oxide systems is critical to their progress and application. In this work, we study the interplay among electron and phonon thermal transport, mass-impurity scattering, and phonon-vacancy interactions on the thermal conductivity of cadmium oxide. We use time domain thermoreflectance to measure the thermal conductivity of a set of CdO thin films doped with Dy up to the saturation limit. Using measurements at room temperature and 80 K, our results suggest that the enhancement in thermal conductivity at low Dy concentrations is dominated by an increase in the electron mobility due to a decrease in oxygen vacancy concentration. Furthermore, we find that at intermediate doping concentrations, the subsequent decrease in thermal conductivity can be ascribed to a large reduction in phononic thermal transport due to both point defect and cation-vacancy scattering. With these results, we gain insight into the complex dynamics driving phonon scattering and resulting thermal transport in functional oxides. © 2016 AIP Publishing LLC.

[<http://dx.doi.org/10.1063/1.4939652>]

Functional oxides are a class of materials that offer highly tunable optical, mechanical, and transport properties. Advancements in materials and processing have led to functional oxides being central to applications such as microelectronics,^{1–3} plasmonics,^{4–6} photovoltaics,^{7–9} and optics, in general.^{10–12} While the electrical, optical, and mechanical properties of functional oxides have been the center of quite extensive study, thermal properties and the role of defects on these thermal transport properties are often overlooked or misunderstood.

The impact of point defects on phonon dominated thermal transport has been largely addressed by the studies of impurities in silicon and silicon-based materials.^{13–15} Looking towards oxides, the previous works have quantified the role of oxygen vacancy interactions with phonons in bulk materials, starting around the 1960s.^{16–20} With recent advances in materials processing and characterization, a new level of capability and complexity is commonly being utilized in the form of thin film oxide materials. In these thin film systems, nanoscale dimensionality and resulting phonon scattering at boundaries is another aspect of thermal conductivity that has been the subject of many recent investigations.^{21–26} Interest in thermoelectric oxides as a viable source of energy scavenging along with high temperature thermal barrier coatings has encouraged more focus on the ability to reduce thermal transport in oxides based on sample geometry, nanostructure, and stoichiometry. Beyond reduction, it can be even more insightful to tune thermal transport in these materials with the variety of controls available through advanced processing and characterization.

In our previous study, we demonstrated bi-directional control of the thermal conductivity of doped cadmium oxide (CdO) based on competing electron and phonon contributions to thermal transport.⁶ The observed change was due to an increase in carrier density from doping and a decrease in phonon conduction via impurity scattering. These unique phonon scattering processes that drive the thermal resistances in complex oxides are deeply related to both the impurity and vacancy concentrations. The validation of theoretically derived models that predict this interplay has received little to no attention. The previously studied⁶ Dy doped CdO material system offers experimental understanding into the interrelated role of phonon-defect and phonon-vacancy scattering on thermal conductivity in oxides.

In this work, we study the thermal conductivity of a series of thin CdO films doped with Dy and isolate the role of phonon-vacancy scattering on thermal conductivity. We demonstrated in our previous work that bi-directional tuning of thermal conductivity in CdO is achievable via Dy doping.⁶ We use time-domain thermoreflectance (TDTR) to measure the thermal conductivity of CdO thin films at room temperature and 80 K in order to experimentally identify the role of phonon-vacancy scattering on this bi-directional tuning of thermal conduction in CdO. Our data show that the behavior of the phonon and electron dominated thermal carrier regimes differ based on temperature, while the various point defect interactions obey relatively well-known trends exhibited in the literature.^{27,28} By the mechanism of our 80 K thermal conductivity measurements, we are able to identify the influence of phonon-vacancy scattering on thermal conductivity, providing direct validation of previously derived models for phonon-vacancy scattering rates. Our analyses

^{a)}Electronic mail: phopkins@virginia.edu

suggest that enhancement in thermal conductivity at low Dy concentrations is dominated by an increase in the electron mobility due to a decrease in oxygen vacancies, while the reduction in thermal conductivity at intermediate doping concentrations is partially driven by phonon scattering from cation vacancies.

The CdO:Dy films were synthesized via plasma assisted molecular beam epitaxy. Heteroepitaxial films with thicknesses of 500 nm were grown on MgO (100) substrates. Dysprosium acts as an n-type dopant, replacing Cd atoms on the Cd site of the CdO crystal. Doping with Dy encourages a reduction in oxygen vacancies in the CdO via Fermi-level pinning.⁶ This results in a shift of the defect equilibrium to a state with a fixed substitutional impurity concentration. Considering that the difference in radius due to substitution of Dy on a Cd site is much less than that of a vacancy in an O site, the initial introduction of Dy into the system is accompanied with an increase in carrier mobility.⁶

Thermal conductivity measurements were performed using TDTR, an optical pump-probe technique used commonly to measure nanoscale thermal transport phenomena.^{29–31} In our experiment, we use an 80 MHz Ti:sapphire oscillator emitting a train of 800 nm wavelength, sub-picosecond pulses, which are split into a modulated pump for thermal excitation and a time-delayed probe to measure the temporal change in surface reflectivity at the pump modulation frequency. The measured decay in the reflected probe signal is fit to a thermal model that is used to determine the thermal conductivities of the CdO films.^{29–31} In these experiments, we use an Al thermal transducer with a thickness of 83 ± 3 nm, and a pump and probe spot radii of $42 \mu\text{m}$ and $11 \mu\text{m}$, respectively. We assume literature values for the heat capacities of the Al,³² CdO,³³ MgO,³⁴ and thermal conductivity of the MgO.³⁵ The major source of error in our analysis arises from uncertainty in the thickness of the Al transducer. To minimize this uncertainty, we verify the Al film thickness with both X-ray reflectivity and picosecond acoustic analyses.^{36,37}

In order to understand the physical mechanisms affecting the measured thermal conductivities in these materials, we conduct measurements at 80 K to compare to our previous measurements reported at room temperature.⁶ The results seen in Fig. 1 show the measured thermal conductivity of CdO:Dy as a function of Dy concentration both at room temperature⁶ and at 80 K. The room temperature data transition through a number of regions of dominant scattering mechanisms. Initially, in region “R1” of Fig. 1, the addition of Dy results in a decrease in oxygen vacancies, thus decreasing the total scattering of thermal carriers and increasing the total thermal conductivity. In the second region, “R2,” the Dy concentration is high enough to significantly scatter the thermal carriers (i.e., both electrons and phonons) in the system and the only contribution acting to increase the thermal conductivity is the addition of free carriers from doping. The final data point in this region (0.08 at. % Dy) represents the maximum electrical contribution to the thermal conductivity, κ_{elec} , which leads to a second peak for the measured thermal conductivity at room temperature. The electrical contribution to the thermal conductivity was calculated using the Wiedemann-Franz law applied to our electrical resistivity measurements on these

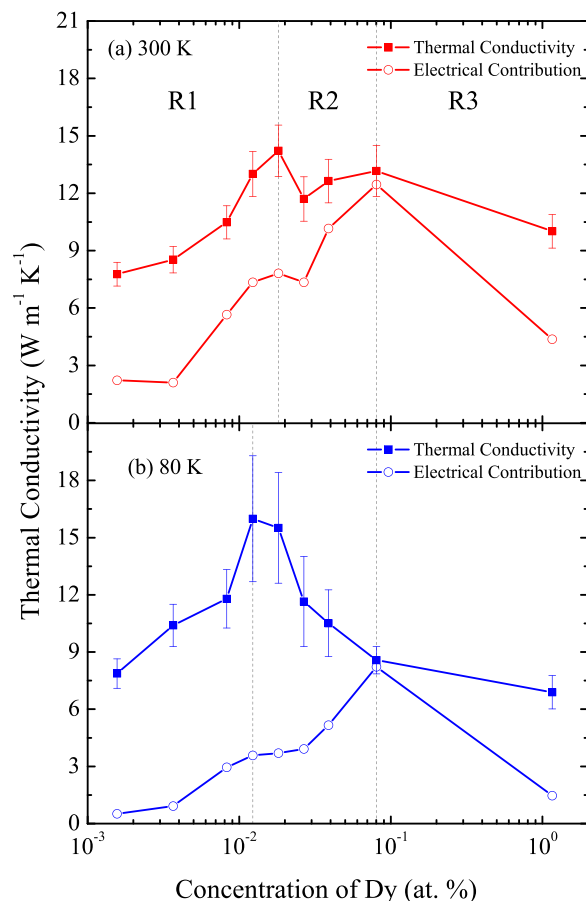


FIG. 1. Measured thermal conductivity of CdO:Dy for various Dy concentrations. Squares and circles indicate the total measured thermal conductivity and the calculated electronic contribution to thermal conductivity, respectively. Measurements were taken at (a) 300 K and (b) 80 K. Included are delineations between regions in which the total thermal conductivity is driven by R1: a decrease in the scattering of the thermal carriers; R2: an increase in phonon scattering balanced by an increase in electrical carrier population; and R3: an increase in electron and phonon scattering that overwhelms additional increase in the electrical carrier population.

samples.⁶ In the final region, “R3,” the Dy concentration is high enough to effectively scatter all carriers and the total thermal conductivity decreases. This final region includes data from near the solubility limit of Dy in CdO, giving us an upper bound on the defect interactions, and we can not rule out the formation of secondary phases at this concentration.

In Fig. 1(b), we see a slight shift in these regions and changes in the trends of thermal conductivity as a function of Dy concentration. This variation of thermal characteristics with temperature is crucial to understanding the dominant thermal transport mechanisms being affected in each region. We see that “R1,” delineated by the total peak in the thermal conductivity, has shifted slightly, which can be understood by a change in the phonon population; at low temperatures, we expect less high frequency phonons which are more impacted by point defect scattering. In addition, at low temperatures, the second peak in the thermal conductivity is no longer present, since this peak is due to the electrical contribution to the thermal conductivity, which is significantly reduced at low temperatures.

To understand the effects of changes in various defect populations on the phonon thermal conductivity in CdO, we subtract the electronic contribution from the total measured thermal conductivity and analyze the phonon thermal

conductivity, modeled by $\kappa_{ph} = C_v v^2 \tau / 3$, where C_v is the heat capacity, v is the phonon velocity, and τ is the overall scattering time given in Eq. (1). In this material system, we expect contributions to the phonon thermal resistance from anharmonic interactions, τ_{ph} , baseline impurity scattering, τ_{Imp} , boundary scattering, τ_{Bound} , dopant scattering, τ_{Def} , and vacancy scattering, τ_{Vac} . This is combined via Matthiessen's rule, given by

$$\frac{1}{\tau} = \frac{1}{\tau_{Ph}} + \frac{1}{\tau_{Imp}} + \frac{1}{\tau_{Bound}} + \frac{1}{\tau_{Def}} + \frac{1}{\tau_{Vac}}. \quad (1)$$

We use the literature data to determine the heat capacity and phonon velocities as a function of wavelength from the acoustic branches of the phonon dispersion curve.³⁸ This allows us to use the data obtained in this study to determine the nature of the major phonon scattering mechanisms introduced by doping CdO with Dy. Since the optical branches have a very low corresponding group velocity, the associated thermal conductivity is negligible, and we ignore them in our model.

We expect that the scattering effects from phonon-phonon scattering, baseline impurity scattering, and film boundary scattering to be unchanged with doping. To this extent, we calibrate our scattering parameters using the literature data for phonon-phonon scattering³⁹ and the undoped CdO film of our sample set for baseline impurity and film boundary scattering. We note that Lindsay and Parker⁴⁰ recently modeled the measured thermal conductivity data reported in Ref. 6 using first-principles calculations accounting for anharmonic phonon scattering; the agreement between the calculations and data support our use of the data reported in Ref. 6 to account for the intrinsic phonon-phonon scattering mechanisms in CdO. We use a least squares optimization to fit the baseline impurity and boundary scattering parameters to the measured thermal conductivity of the undoped sample, found in Fig. 2.

With these aspects of the behavior of the thermal conductivity of CdO films quantified, we investigate the effects of Dy doping on phonon scattering to gain more insight into

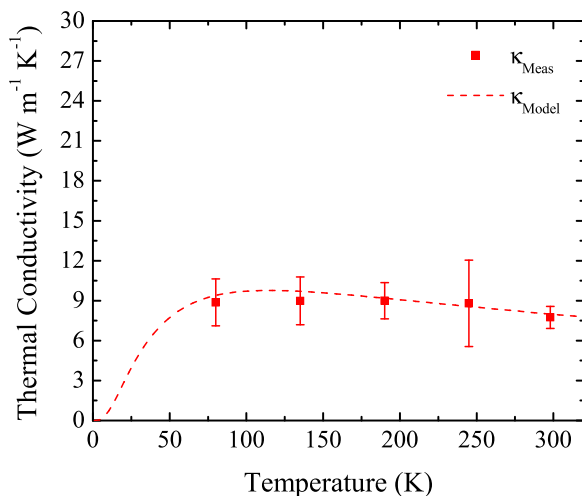


FIG. 2. Measured thermal conductivity as a function of temperature of the undoped film for calibration of the model of thermal conductivity of CdO thin films (dashed line).

the physics of the phonon-vacancy interaction. The form of phonon scattering from impurities is relatively well known, taking the following analytical representation:⁴¹

$$\tau_{Def}^{-1} = A\omega^4 x_{Def} \left[\left(\frac{\Delta M_{Def}}{M_{Host}} \right)^2 + 2 \left[\left(\frac{\Delta G_{Def}}{G_{Host}} \right) - 6.4\gamma \left(\frac{\Delta \delta_{Def}}{\delta_{Host}} \right) \right]^2 \right], \quad (2)$$

where A is a parameter determined by the lattice constant and phonon group velocity of the material, ω is the phonon frequency, and x_{Def} is the concentration of a given defect. The squared terms represent the scattering characteristics due to the mass change and strain change from a defect in the lattice. The mass difference is determined by the change in mass of the defect from the host, ΔM_{Def} divided by the average atomic mass of the host, M_{Host} . The strain difference is determined using similar factors where ΔG_{Def} is the change in bond stiffness, $\Delta \delta_{def}$ is the change in lattice parameter, and γ is the Grüneisen parameter⁴¹ taken from the literature.⁴² In the case of a vacancy, the factor accounting for the mass change takes the following form to account for potential energy differences with the absence of an atom:⁴³

$$\frac{\Delta M_{Vac}}{M_{Host}} = -\frac{M_{Vac}}{M_{Host}} - 2, \quad (3)$$

where M_{Vac} is the mass of the missing atom.

Using these formalisms for phonon scattering with impurities and vacancies, we begin by modeling the thermal conductivity of the measured CdO films given with known concentrations of Dy and assuming a concentration of oxygen vacancies from the electrical conductivity of the undoped films. This oxygen vacancy concentration is estimated to be $2 \times 10^{19} \text{ cm}^{-3}$, and decays an order of magnitude due to the Dy doping.⁶ This initial model assumes that the major changing defects in the films are only the Dy dopants and the oxygen vacancies.

This model, labeled as the ‘‘Dy Dominated’’ model in Fig. 3, captures the region ‘‘R1’’ data rather well. The data shown in Fig. 3 are the measured thermal conductivity with the calculated electrical contribution subtracted away, leaving only the phonon thermal conductivity. It is interesting to note in this model that the predicted thermal conductivity is relatively insensitive to phonon scattering with oxygen vacancies. For example, neglecting oxygen vacancies all together results in only a 25% difference in the thermal conductivity at low Dy concentrations and less than a 10% change in model prediction as the doping level exceeds 10^{-2} at. %.

The Dy dominated model fails to capture the phonon thermal conductivity data at higher Dy doping concentrations (region ‘‘R2’’), where we expect dopant scattering to dominate. To understand this, we turn to the literature findings that suggest that, in highly doped oxide systems, substitutional dopants can be compensated by other vacancy mechanisms in order to reduce the overall energy of the system.^{44,45} In accordance with these findings, we investigate the phonon scattering effects of Cd vacancies with populations dictated by the substitutional doping concentration and

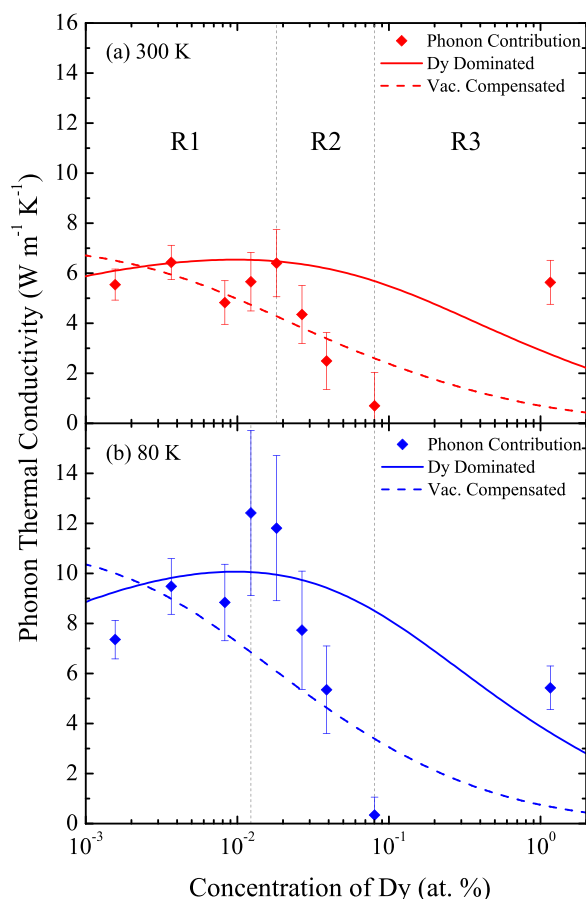


FIG. 3. Phonon thermal conductivity of CdO:Dy at (a) 300 K and (b) 80 K along with bounding models for a system dominated by scattering from Dy doping (solid lines: “Dy Dominated”) and a model for a system with additional scattering from vacancies with concentrations pinned by the Dy concentration (dashed lines: “Vac. Compensated”).

update the model with a Cd vacancy scattering term in the form of Eq. (2). This model, referred to in Fig. 3 as the “Vac. Compensated” model, agrees with the measured data significantly better at the higher Dy concentrations than the “Dy Dominated” model. This agreement, along with similar findings in other oxide systems found in the literature,^{44,45} serves to indicate that there may be an introduction of other point defects compensating the Dy dopants at these high doping concentration levels, and it is these compensating defects that drastically drive the phonon thermal conductivity down.

The highest doping concentration measured in region “R3” does not follow this continued downward trend in the phonon thermal conductivity. This is understood when considering that this sample is near the solubility of Dy in CdO and our characterization indicates that secondary phases have formed.⁶ In this case, there are likely multiple regions that will behave more similarly to dilute solutions of Dy in CdO rather than highly doped solutions. This hypothesis is supported by the relative agreement with the “Dy Dominated” model compared with the “Vacancy Compensated” model. Further characterization of the precipitated phases and their respective Dy concentrations would need to be carried out in order to verify this hypothesis, but is beyond the scope of this study.

There are a number of other components that may be at play to dictate the phonon thermal conductivity of these

films, such as minority defect populations, contributions to the thermal conductivity from optical phonons, and phonon drag from the free electrons in the system.⁴⁶ However, the agreement between the relatively simple models presented in this work and the data measured in this and our previous work⁶ suggest that we have identified the major phonon scattering mechanisms in these materials. Furthermore, agreement of the model and the measured data in the various regimes of Dy doping suggest that the phonon thermal conductivity, and analytical modeling thereof, can be used to identify signs of complex defect interactions in functional oxides. The two models, one taking into account only the known defects and the other identifying the remaining scattering sites, serve as bounds for the major phonon scattering mechanisms in this material and significantly aids in the understanding of the phonon-related thermal conductivity tuning of CdO using Dy dopants.

In conclusion, the CdO:Dy material system illustrates intricate bi-directional tunability of thermal conductivity in complex oxide materials, offering potential next steps for thermal engineering using functional oxides. We have shown that with the introduction of Dy dopants, the thermal conductivity of CdO can be increased or decreased via the interplay among the electronic contribution to thermal conductivity and thermal carrier scattering due to mass-impurity and vacancy concentrations present in the system. Decreasing of the intrinsic oxygen vacancy concentrations increases the electronic mobility, leading to an increase in thermal conductivity at low Dy doping levels, but has a limited effect on the phonon thermal conductivity. At higher Dy doping levels, the lattice thermal conductivity is impacted. Using measurements at multiple temperatures, we are able to formulate a model for the phonon thermal conductivity that highlights the major scattering mechanisms present in the system including mass-impurity and vacancy scattering. We show that Dy mass-impurities contribute to thermal scattering at low Dy concentrations, as expected. However, at higher Dy concentrations, additional defects, namely, cation vacancies, must be taken into account to capture the trend in the data. This results in models which act as bounds for the measured data as the system transitions from dilute dopant scattering to scattering due to both dopant and vacancies at high Dy concentrations.

We appreciate the funding from the Office of Naval Research under Grant No. N00014-15-12769 and Air Force Office of Scientific Research under Grant No. FA9550-14-1-0067.

¹E. H. Nicollian and J. R. Brews, *MOS (Metal Oxide Semiconductor) Physics and Technology* (Wiley, New York, 1982), Vol. 1987.

²B. H. Lee, L. Kang, R. Nieh, W.-J. Qi, and J. C. Lee, “Thermal stability and electrical characteristics of ultrathin hafnium oxide gate dielectric reoxidized with rapid thermal annealing,” *Appl. Phys. Lett.* **76**(14), 1926–1928 (2000).

³K. Nomura, H. Ohta, K. Ueda, T. Kamiya, M. Hirano, and H. Hosono, “Thin-film transistor fabricated in single-crystalline transparent oxide semiconductor,” *Science* **300**(5623), 1269–1272 (2003).

⁴G. V. Naik, J. Kim, and A. Boltasseva, “Oxides and nitrides as alternative plasmonic materials in the optical range,” *Opt. Mater. Express* **1**(6), 1090–1099 (2011).

⁵A. K. Pradhan, R. M. Mundle, K. Santiago, J. R. Skuza, B. Xiao, K. D. Song, M. Bahoura, R. Cheaito, and P. E. Hopkins, “Extreme tunability in

- aluminum doped zinc oxide plasmonic materials for near-infrared applications," *Sci. Rep.* **4**, 6415 (2014).
- ⁶E. Sachet, C. T. Shelton, J. S. Harris, B. E. Gaddy, D. L. Irving, S. Curtarolo, B. F. Donovan, P. E. Hopkins, P. A. Sharma, A. L. Sharma, J. Ihlefeld, S. Franzen, and J.-P. Maria, "Dysprosium-doped cadmium oxide as a gateway material for mid-infrared plasmonics," *Nat. Mater.* **14**(4), 414–420 (2015).
- ⁷A. Hagfeldt and M. Grätzel, "Molecular photovoltaics," *Acc. Chem. Res.* **33**(5), 269–277 (2000).
- ⁸C. J. Barbé, F. Arendse, P. Comte, M. Jirousek, F. Lenzmann, V. Shklover, and M. Grätzel, "Nanocrystalline titanium oxide electrodes for photovoltaic applications," *J. Am. Ceram. Soc.* **80**(12), 3157–3171 (1997).
- ⁹P. Ravirajan, A. M. Peiró, M. K. Nazeeruddin, M. Graetzel, D. D. C. Bradley, J. R. Durrant, and J. Nelson, "Hybrid polymer/zinc oxide photovoltaic devices with vertically oriented ZnO nanorods and an amphiphilic molecular interface layer," *J. Phys. Chem. B* **110**(15), 7635–7639 (2006).
- ¹⁰M. J. Weber, *Handbook of Optical Materials* (CRC Press, 2002), Vol. 19.
- ¹¹S. R. Marder, J. E. Sohn, and G. D. Stucky, "Materials for nonlinear optics chemical perspectives," Technical report (Report # 455), DTIC Document, 1991.
- ¹²A. B. Djurišić and Y. H. Leung, "Optical properties of ZnO nanostructures," *Small* **2**(8–9), 944–961 (2006).
- ¹³M. Asheghi, M. N. Touzelbaev, K. E. Goodson, Y. K. Leung, and S. S. Wong, "Temperature-dependent thermal conductivity of single-crystal silicon layers in SOI substrates," *J. Heat Transfer* **120**(1), 30–36 (1998).
- ¹⁴G. H. Zhu, H. Lee, Y. C. Lan, X. W. Wang, G. Joshi, D. Z. Wang, J. Yang, D. Vashaev, H. Guilbert, A. Pillitteri, M. S. Dresselhaus, G. Chen, and Z. F. Ren, "Increased phonon scattering by nanograins and point defects in nanostructured silicon with a low concentration of germanium," *Phys. Rev. Lett.* **102**, 196803 (2009).
- ¹⁵Y. Lee, S. Lee, and G. S. Hwang, "Effects of vacancy defects on thermal conductivity in crystalline silicon: A nonequilibrium molecular dynamics study," *Phys. Rev. B* **83**, 125202 (2011).
- ¹⁶P. G. Klemens, "The scattering of low-frequency lattice waves by static imperfections," *Proc. Phys. Soc. A* **68**(12), 1113 (1955).
- ¹⁷P. G. Klemens, "Thermal resistance due to point defects at high temperatures," *Phys. Rev.* **119**, 507–509 (1960).
- ¹⁸W. R. Thurber and A. J. H. Mante, "Thermal conductivity and thermoelectric power of rutile (TiO₂)," *Phys. Rev.* **139**, A1655–A1665 (1965).
- ¹⁹H. J. Siebeneck, W. P. Minnear, R. C. Bradt, and D. P. H. Hasselman, "Thermal diffusivity of nonstoichiometric titanium dioxide," *J. Am. Ceram. Soc.* **59**(1–2), 84 (1976).
- ²⁰C. A. Ratsifaritana and P. G. Klemens, "Scattering of phonons by vacancies," *Int. J. Thermophys.* **8**(6), 737–750 (1987).
- ²¹P. G. Klemens, "Theory of thermal conduction in thin ceramic films," *Int. J. Thermophys.* **22**(1), 265–275 (2001).
- ²²B. F. Donovan, B. M. Foley, J. F. Ihlefeld, J.-P. Maria, and P. E. Hopkins, "Spectral phonon scattering effects on the thermal conductivity of nano-grained barium titanate," *Appl. Phys. Lett.* **105**(8), 082907 (2014).
- ²³B. M. Foley, H. J. Brown-Shaklee, J. C. Duda, R. Cheaito, B. J. Gibbons, D. Medlin, J. F. Ihlefeld, and P. E. Hopkins, "Thermal conductivity of nano-grained SrTiO₃ thin films," *Appl. Phys. Lett.* **101**(23), 231908 (2012).
- ²⁴J. F. Ihlefeld, B. M. Foley, D. A. Scrymgeour, J. R. Michael, B. B. McKenzie, D. L. Medlin, M. Wallace, S. Trolrier-McKinstry, and P. E. Hopkins, "Room-temperature voltage tunable phonon thermal conductivity via reconfigurable interfaces in ferroelectric thin films," *Nano Lett.* **15**(3), 1791–1795 (2015).
- ²⁵J. Ravichandran, A. K. Yadav, R. Cheaito, P. B. Rossen, A. Soukiasian, S. J. Suresha, J. C. Duda, B. M. Foley, C.-H. Lee, Y. Zhu, A. W. Lichtenberger, J. E. Moore, D. A. Muller, D. G. Schlom, P. E. Hopkins, A. Majumdar, R. Ramesh, and M. A. Zurbuchen, "Crossover from incoherent to coherent phonon scattering in epitaxial oxide superlattices," *Nat. Mater.* **13**(2), 168–172 (2014).
- ²⁶M. N. Luckyanova, D. Chen, W. Ma, H. L. Tuller, G. Chen, and B. Yildiz, "Thermal conductivity control by oxygen defect concentration modification in reducible oxides: The case of Pr_{0.1}Ce_{0.9}O_{2-δ} thin films," *Appl. Phys. Lett.* **104**(6), 061911 (2014).
- ²⁷C. Kittel and P. McEuen, *Introduction to Solid State Physics* (Wiley, New York, 1986), Vol. 8.
- ²⁸P. G. Klemens, "Phonon scattering by oxygen vacancies in ceramics," *Phys. B: Condens. Matter* **263–264**, 102–104 (1999).
- ²⁹D. G. Cahill, "Analysis of heat flow in layered structures for time-domain thermoreflectance," *Rev. Sci. Instrum.* **75**(12), 5119–5122 (2004).
- ³⁰P. E. Hopkins, J. R. Serrano, L. M. Phinney, S. P. Kearney, T. W. Grasser, and C. T. Harris, "Criteria for cross-plane dominated thermal transport in multilayer thin film systems during modulated laser heating," *J. Heat Transfer* **132**(8), 081302 (2010).
- ³¹A. J. Schmidt, X. Chen, and G. Chen, "Pulse accumulation, radial heat conduction, and anisotropic thermal conductivity in pump-probe transient thermoreflectance," *Rev. Sci. Instrum.* **79**(11), 114902 (2008).
- ³²G. T. Furukawa, M. L. Reilly, and J. S. Gallagher, "Critical analysis of heat-capacity data and evaluation of thermodynamic properties of ruthenium, rhodium, palladium, iridium, and platinum from 0 to 300 K," *J. Phys. Chem. Ref. Data* **3**, 163 (1974).
- ³³O. Madelung, U. Rössler, and M. Schulz, "Cadmium oxide (CdO) debye temperature, heat capacity, melting point, density," in *II-VI and I-VII Compounds; Semimagnetic Compounds, volume 41B of Landolt-Börnstein - Group III Condensed Matter*, edited by O. Madelung, U. Rössler, and M. Schulz (Springer, Berlin, Heidelberg, 1999), pp. 1–3.
- ³⁴M. W. Chase, "NIST-JANAF thermochemical tables," in *Journal of Physical and Chemical Reference Data*, 4th ed. (National Institute of Standards and Technology, 1998), Vol. 1.
- ³⁵G. A. Slack, "Thermal conductivity of MgO, Al₂O₃, MgAl₂O₄, and Fe₃O₄ crystals from 3 to 300 K," *Phys. Rev.* **126**, 427–441 (1962).
- ³⁶C. Thomsen, J. Strait, Z. Vardeny, H. J. Maris, J. Tauc, and J. J. Hauser, "Coherent phonon generation and detection by picosecond light pulses," *Phys. Rev. Lett.* **53**, 989–992 (1984).
- ³⁷C. Thomsen, H. T. Grahn, H. J. Maris, and J. Tauc, "Surface generation and detection of phonons by picosecond light pulses," *Phys. Rev. B* **34**, 4129–4138 (1986).
- ³⁸L. Narasimha, A. Kandala, J. B. B. Rayappan, J. B. Gopalakrishnan, S. M. G. Manasai, and L. Nallathambi, "Effect of least variations in the lattice constant in the lattice dynamics of nanostructured CdO," *J. Appl. Sci.* **12**, 1726 (2012).
- ³⁹Q. Lü, S. F. Wang, L. J. Li, J. L. Wang, S. Y. Dai, W. Yu, and G. S. Fu, "Electrical and thermal transport properties of CdO ceramics," *Sci. China: Phys., Mech. Astron.* **57**, 1–5 (2014).
- ⁴⁰L. Lindsay and D. S. Parker, "Calculated transport properties of CdO: Thermal conductivity and thermoelectric power factor," *Phys. Rev. B* **92**, 144301 (2015).
- ⁴¹B. Abeles, "Lattice thermal conductivity of disordered semiconductor alloys at high temperatures," *Phys. Rev.* **131**, 1906–1911 (1963).
- ⁴²B. D. Sahoo, K. D. Joshi, and S. C. Gupta, "Ab initio calculations on structural, elastic and dynamic stability of CdO at high pressures," *J. Appl. Phys.* **112**(9), 093523 (2012).
- ⁴³P. G. Klemens, "Theory of heat conduction in nonstoichiometric oxides and carbides," *High Temp. - High Pressures* **17**(1), 41–45 (1985).
- ⁴⁴P. Kofstad, *Nonstoichiometry, Diffusion, and Electrical Conductivity in Binary Metal Oxides* (Wiley-Interscience, New York, 1972).
- ⁴⁵J. Nowotny, T. Bak, M. K. Nowotny, and L. R. Sheppard, "Defect chemistry and electrical properties of titanium dioxide. 1. Defect diagrams," *J. Phys. Chem. C* **112**(2), 590–601 (2008).
- ⁴⁶B. Liao, B. Qiu, J. Zhou, S. Huberman, K. Esfarjani, and G. Chen, "Significant reduction of lattice thermal conductivity by electron-phonon interaction in silicon with high carrier concentrations: A first-principles study," *Phys. Rev. Lett.* **114**, 115901 (2015).